Journal of Molecular Graphics and Modelling 29 (2011) 643–649

Contents lists available at ScienceDirect

Journal of Molecular Graphics and Modelling

journal homepage: www.elsevier.com/locate/JMGM

Free energy perturbation approach for the rational engineering of the antibody for human hepatitis B virus

Hwangseo Park[a,*], Young Ho Jeon[b,c,**]

[a] Department of Bioscience and Biotechnology, Sejong University, 98 Kunja-Dong, Kwangjin-Ku, Seoul 143-747, Republic of Korea
[b] Division of Magnetic Resonance, Korea Basic Science Institute, 804-1 Yangchung-Ri, Ochang, Chungbuk 363-883, Republic of Korea
[c] Bio-Analytical Science Program, University of Science and Technology, Daejeon 350-333, Republic of Korea

ARTICLE INFO

Article history:
Received 30 September 2010
Received in revised form
10 November 2010
Accepted 15 November 2010
Available online 23 November 2010

Keywords:
Free energy perturbation
Molecular dynamics
Antibody engineering
Mutation
Protein–protein interaction

ABSTRACT

HzKR127 is the humanized monoclonal antibody effective for the neutralization of human hepatitis B virus. By means of the free energy perturbation (FEP) calculations based on molecular dynamic (MD) simulations, we examine the mutation-induced variations in the energetic and structural features associated with the interactions between HzKR127 and its antigen. N58A, Y96A, D97A, and D97A/Y102A mutants of HzKR127 are taken in account in this study for which the experimental data for relative efficacies with respect to the wild-type antibody are available. The results of the present MD–FEP simulation studies show that in order to enhance the affinity for the antigen, the engineering of HzKR127 should be made in such a way as to promote the dynamic stability of the overall protein conformation and that of the translational motion of the antigen in the antibody–antigen complex. The relative binding free energies of the four mutant antibodies obtained from MD–FEP calculations compare pretty well with the experimental mutagenesis data with the associated squared correlation coefficient of 0.96. This indicates that MD–FEP calculations may serve as a useful computational tool for rational antibody engineering. Discussed in detail are the differences in the structural features of antibody–antigen interactions between the wild-type and the mutant antibodies that are responsible for the change in binding affinities for the antigen.

1. Introduction

Many acute and chronic liver diseases stem from the infection by human hepatitis B virus (HBV). HBV infection has been distributed worldwide to the extent that four millions of global population are the carrier of HBV. It is a small enveloped DNA virus whose envelope contains three types of surface glycoproteins including large (L), middle (M), and small (S) proteins [1]. Three domains of the envelope protein named preS1, preS2, and S are consecutively located in the HBV genome. The translations of S, preS2 & S, and preS1 & preS2 & S domains lead to the formations of S, M, and L proteins, respectively [2]. Among these, L protein is responsible for the viral infection with its preS1 domain playing a crucial role in the cell attachment that precedes the invasion of the virus in the host cell [3]. The region of residues 21–47 in preS1 has been of particular interest because it was shown to be a specific binding site for hepatocyte receptors and therefore considered as the epitope for designing the virus-neutralizing agents [4].

The murine monoclonal antibody (mAb) KR127 is known to specifically bind to the preS1 domain (residues 37–45) of HBV. The humanized version of KR127 antibody (HzKR127) is also capable of binding to the preS1 domain. Furthermore, it has been shown to reveal a broad neutralizing activity in chimpanzee, which has an effect of protecting the chimpanzee from the HBV infection. HzKR127 can thus serve as the potential for immunoprophylaxis of HBV infection [5,6].

Humanized antibody can be constructed by the graft of the complementarity-determining regions (CDRs) of murine mAb onto the human framework regions (FRs), which is referred to as CDR grafting [7]. Clinical studies indicated that the humanized antibody has less immunogenicity than murine monoclonal and chimeric antibodies [8]. However, the humanized antibodies constructed from CDR grafting often has a reduced affinity for the preS1 antigen, because some FR residues directly interact with the transformed CDR loops [9]. To develop the clinically useful humanized antibody, therefore, some FR residues should be replaced with the other fit amino acids that can increase the structural stability of HzKR127 as well as the affinity for the antigen [10,11]. In this

* Corresponding author. Tel.: +82 2 3408 3766; fax: +82 2 3408 4334.
** Corresponding author at: Division of Magnetic Resonance, Korea Basic Science Institute, 804-1 Yangchung-Ri, Ochang, Chungbuk 363-883, Republic of Korea.
E-mail addresses: hspark@sejong.ac.kr (H. Park), yhjeon@kbsi.re.kr (Y.H. Jeon).

1093-3263/$ – see front matter © 2010 Elsevier Inc. All rights reserved.
doi:10.1016/j.jmgm.2010.11.010

regard, a rational protein engineering with computational methods can be helpful for finding the mutants of a humanized antibody with desired physicochemical characteristics. The quantitative and systematic engineering strategies have indeed offered an opportunity to replace the traditional hit-and-miss approach to protein optimization [12–15].

A few years ago, Chi et al. reported the X-ray crystal structure of HzKR127 in complex with a major epitope peptide, which provides a structural basis for the neutralization of HBV [16]. The antibody was shown to undergo an opening of CDR to a substantial extent upon binding of the peptide antigen. To determine the residues that play a key role in virus neutralization, they carried out the extensive alanine-scanning mutageneses for various CDR residues in HzKR127. It was found that the antigen-binding activity of HzKR127 should be significantly impaired by the alanine substitutions on most of the antigen-contacting residues in the heavy and light chains including Trp33H, Asn35H, Arg50H, Glu95H, Tyr96H, Asn28L, Tyr32L, Asn34L, Val89L, Gly91L, Phe94L, and Gln96L [16]. This indicated that most of the direct HzKR127–preS1 interactions observed in the X-ray crystal structure would make a significant contribution to the stabilization of the antibody–antigen complex in a cooperative fashion. Thus, the structural and mutagenesis studies have shed a new light on the rational design of the mutant antibodies with a maximal humanization and an enhanced binding affinity for the antigen.

In the present study, we address the structural and energetic features of the interactions between the preS1 antigen and the wild-type and the mutant forms HzKR127 with varying binding affinities for the antigen based on free energy perturbation (FEP) calculations with molecular dynamic (MD) simulations. Through these comparative analyses of antigen binding, we aim to elucidate not only the relative potencies of the wild-type and mutant antibodies but also various mutational effects on the pattern for the formation of the antibody–antigen complex, which enables to gain insight into designing new antibody drugs with improved potency. The relative binding free energy is computed to estimate the efficacy of a mutant antibody with respect to the wild type. It will be shown that these MD–FEP simulations can be a valuable tool for predicting the mutant antibodies with an increased efficacy, and for identifying the affinity-enhancing factors pertinent to the stabilization of the antigen in CDR of HzKR127.

2. Computational methods

The X-ray crystal structure of HzKR127 in complex with the preS1 antigen (PDB entry 2EH8) [16] was used as the starting point of MD–FEP calculations. Missing heavy atoms and hydrogen atoms were added after removing the crystallographic water molecules. A special attention was paid to assign the protonation states of the ionizable Asp, Glu, His, and Lys residues. The side chains of Asp and Glu residues were assumed to be neutral if one of their carboxylate oxygens pointed toward a hydrogen-bond accepting group including the backbone aminocarbonyl oxygen at a distance within 3.5 Å, a generally accepted distance limit for a hydrogen bond of moderate strength [17]. Similarly, the side chains of Lys residues were protonated unless the NZ atom was in a close proximity of a hydrogen-bond donating group. The same procedure was also applied to determine the protonation states of ND and NE atoms in the side chains of His residues. In this way, Asp70 in the light chain and Lys143 in the heavy chain were found to be neutral whereas the rest of the side chains of Asp, Glu, and Lys residues were ionized. The all-atom models of the wild-type HzKR127 were then transformed with MD–FEP simulations into N58A, Y96A, D97A, and D97A/Y102A mutants to investigate the mutational effects on the variation of the structural and energetic features associated with the antibody–antigen interactions.

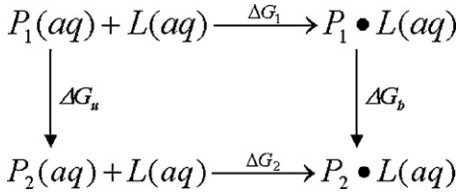

Fig. 1. Thermodynamic cycle used in computing the free energy change in the virtual transformation of wild-type HzKR127 (P_1) into a mutant (P_2) in the resting (ΔG_u) and in the antigen-bound form (ΔG_b), and the relative binding free energy of the antigen L for a mutant HzKR127 with respect to the wild type ($\Delta\Delta G_{bind}$).

In order to compute the change in binding free energy ($\Delta\Delta G_{bind}$) of the antigen in going from the wild-type (P_1) to a mutant HzKR127 (P_2), we employed a simple thermodynamic cycle depicted in Fig. 1. Because free energy is a state function, the sum of all free energy changes in a thermodynamic cycle is zero. Therefore, $\Delta\Delta G_{bind}$ can be expressed as follows:

$$\Delta\Delta G_{bind} = \Delta G_2 - \Delta G_1 = \Delta G_b - \Delta G_u \quad (1)$$

where ΔG_2 and ΔG_1 refer to the binding free energies of P_2 and P_1 for the antigen L, respectively, and ΔG_b and ΔG_u to the free energy changes associated with the virtual transformations of P_1 into P_2 in the antigen-bound and in the resting forms, respectively. We obtained $\Delta\Delta G_{bind}$ by FEP calculations of ΔG_b and ΔG_u from the independent MD simulations of liganded and unliganded forms of HzKR127.

To determine $\Delta\Delta G_{bind}$ between P_1 (initial state, wild type) and P_2 (final state, mutant), the free energy changes involved in the transformation of P_1 into P_2 should be calculated for both the antigen-bound and the resting forms of the antibody. These free energy changes can be computed by perturbing the Hamiltonian of the initial state into the final one. This transformation can be accomplished through a parametrization of the terms comprising the interaction potentials of the system with a change of state variable (λ) that maps the initial and the final states onto 0 and 1, respectively. Fig. 2 illustrates how the structural transformations can be made to obtain a mutant from the wild-type antibody, in the case of the mutation from tyrosine to alanine residue for example.

The total free energy change from the initial to the final state can then be computed by summing the incremental free energy changes over several windows of λ, as it changes from 0 to 1 with the discrete and uniformly spaced intervals:

$$\Delta G = G_1 - G_0 = \sum_i (G_{\lambda(i+1)} - G_{\lambda(i)})$$
$$= -RT \sum_i \ln \left\langle \exp\left(-\left[\frac{V_{\lambda(i+1)} - V_{\lambda(i)}}{RT} \right] \right) \right\rangle_{\lambda(i)} \quad (2)$$

Here, G_0 and G_1 are the free energies of states 0 and 1, respectively. $V_{\lambda(i)}$ represents the potential energy function for the representative state $\lambda_{(i)}$, and $\langle\,\rangle_{\lambda(i)}$ designates the ensemble average of the enclosed quantity for the state $\lambda_{(i)}$.

MD–FEP simulations of HzKR127 and its complex with the preS1 antigen were carried out with the aid of the GIBBS module in AMBER 7 [18] and the force field parameters for proteins reported by Cornell et al. [19], using the X-ray crystal structure reported by Chi et al. [16] as the starting structure. After adding the chloride ions for charge neutralization, the all-atom models for HzKR127 and its antigen-bound form were immersed in rectangular boxes containing about 15,000 TIP3P [20] water molecules. This led to the formation of a rectangular solvent box of dimension 81.1 Å × 74.0 Å × 106.3 Å. After 200 cycles of energy minimization to remove the bad steric contacts, we equilibrated all systems beginning with 20 ps equilibration dynamics of the sol-

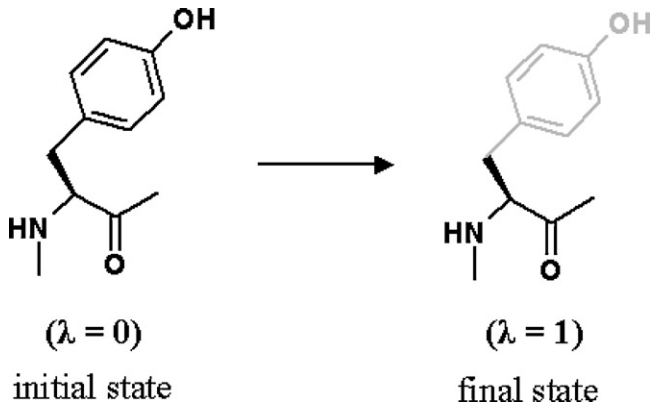

Fig. 2. Structural transformation of the wild type with a tyrosine residue (λ = 0) into a mutant antibody with alanine (λ = 1) at the same position. In this case, the phenyl group in the wild type should be changed to a hydrogen atom.

vent molecules at 300 K. The next step involved the equilibration of the solute with a fixed configuration of the solvent molecules consecutively at 10, 50, 100, 150, 200, 250, and 300 K for 10 ps at each temperature. Then, the equilibration dynamics of the entire system was performed at 300 K for 100 ps.

Following the aforementioned equilibration dynamics, we performed 840 ps of perturbation for each mutation of HzKR127 both in the resting and in the antigen-bound forms. Each perturbation consisted of 21 windows with 20,000 steps of equilibration and 20,000 steps of data collection. In these MD-based FEP calculations, a periodic boundary condition was employed in the NPT ensemble at 300 K using Berendsen temperature coupling [21] and constant pressure (1 atm) with isotropic molecule-based scaling. The SHAKE algorithm [22] with a tolerance of 10^{-6} Å was applied to fix all bond lengths involving the hydrogen atom. We used a time step of 1 fs and a nonbonded-interaction cutoff radius of 12 Å. A doublewide sampling procedure was performed for all of the structural transformations, and the reported results were based on the averages from the backward and forward simulations. Although a significant advancement has been made in sampling with the replica-exchange methodology [23], the classical method was employed in this study due to a technical difficulty in implementing the new algorithm. As an estimation of the statistical error, we used half the difference between the absolute values of forward and reverse free energy changes, and the error in $\Delta\Delta G_{bind}$ was calculated as the square root of the sum of the individual errors in ΔG_u and ΔG_b.

3. Results and discussion

N58A, Y96A, D97A, and D97A/Y102A mutants of the HzKR127 antibody were selected to investigate the mutational effects on the variations of the energetic and structural features in the interaction with the preS1 antigen. The reasons for the choice of these four mutants in the present MD–FEP calculations lie in that all of the mutation sites are located in the heavy chain around the binding pocket comprising the CDR loops to accommodate the antigen, and the experimental data on the binding affinities for the antigen are available. Therefore, the comparison of the complexation patterns of wild-type and mutant antibodies for the preS1 antigen would be informative for designing a new affinity-enhancing mutant antibody for neutralizing HBV.

As a check for the reliability of the present MD–FEP simulations, we examined if the protein structures in the resting and in the antigen-bound forms of HzKR127 would remain stable under the simulation conditions described in the previous section. For this purpose, we calculated the root-mean-square-deviations from the starting structures ($RMSD_{init}$) for all C_α atoms of HzKR127 during the MD–FEP calculations for the four mutations under consideration. As shown in Fig. 3, the $RMSD_{init}$ values remain within 2.5 and 2.2 Å in the resting and in the antigen-bound forms of HzKR127, respectively. The lower $RMSD_{init}$ values in the latter indicate that the binding of antigen would have an effect of reducing the amplitude in the conformational motion of HzKR127. In both bound and unbound simulations, the $RMSD_{init}$ values for the mutation from the wild type to Y96A mutant appear to be dynamically most unstable, which may be related with its lowest binding affinity for the preS1 antigen among the four mutants under investigation [16]. It is also noted that the $RMSD_{init}$ values reveal a convergent behavior with respect to the simulation time in bound and unbound simulations irrespective of the mutation types, which indicates the maintenance of protein conformation in a stable fashion during the entire course of free energy simulations. This result is consistent with the previous mutagenesis studies that demonstrated the insignificant mutational effects of the antigen-binding region on the structural stability of HzKR127 [16]. Judging from the dynamic stabilities of the protein conformation in bound and unbound simulations, it is expected that the calculated free energy differences should be due to the structural perturbations in the side chains around the CDR loops and the resulting changes in the antibody–antigen interactions instead of some unwanted large conformational changes in the antibody.

Shown in Fig. 4 are the time dependences of $RMSD_{init}$ values for all heavy atoms of the preS1 antigen bound in CDR of the wild-type and mutant antibodies. We note that the $RMSD_{init}$ values of the antigen fall into 1.5 Å during the entire course of simulation in all four cases. These dynamic stabilities of ligand positions further support the reasonableness of the simulation conditions described in the previous section. The lower $RMSD_{init}$ values of the antigen than those of the antibody C_α atoms suggests that the positional shift of the antigen within CDR should be restricted when compared to the conformational change of the antibody, which is not surprising for the nanomolar binding affinity of the antigen to the antibody [16].

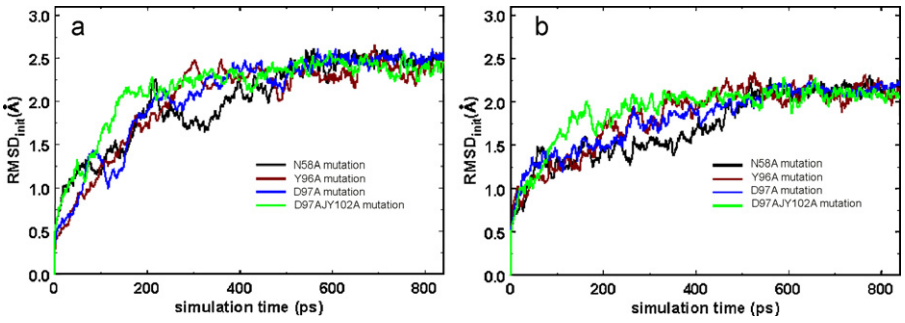

Fig. 3. Time dependences of the root mean square deviations of backbone C_α atoms from the initial structures ($RMSD_{init}$) during MD–FEP simulations of HzKR127 antibody (a) in the resting form and (b) in complex with the preS1 antigen.

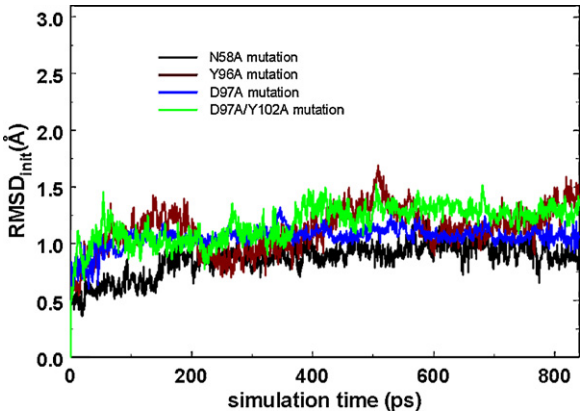

Fig. 4. Time dependences of the $RMSD_{init}$ values for all heavy atoms of the preS1 antigen during the structural transformation from the wild type to a mutant antibody with MD–FEP simulations.

The positions of the antigen appear to be dynamically most unstable in the mutation from the wild type to Y96A mutant, indicating that the variations in the interaction between the HzKR127 and the antigen should be most significant in this mutation. This is consistent with the largest conformational change of the protein conformation in the same mutation (Fig. 3). Thus, the dynamic properties computed during the structural transformation from the wild type to Y96A mutant indicate a destabilization of the antibody–antigen complex, which is not the case for the other three mutations under investigation.

As described in the previous section, we apply the FEP protocol to get the relative binding free energies of the mutant antibodies with respect to the wild-type. The changes in free energy of binding for each λ interval are shown in Fig. 5 for the four mutations under consideration. The binding free energies appear to increase or decrease linearly with the increase of λ, and exhibit a convergent behavior at the end of simulation both for antigen-free and for antigen-bound forms of HzKR127. This confirms the dynamic stability of MD/FEP simulations with respect to the structural transformations of the wild-type HzKR127 into the mutants. Summarized in Table 1 are the calculated relative binding free energies and its components in comparison with the corresponding experimental data. In agreement with the previous experimental results, our FEP calculations indicate an increase in the binding affinities of N58A, D97A, and D97A/Y102A mutants of HzKR127 for the preS1 antigen. They are also consistent with the experimental implication that Y96A mutant of HzKR127 has a lower binding affinity than the wild type. ΔG_u and ΔG_b appear to become positive with the change of Asn58 or Tyr96 in the heavy chain of HzKR127 to the alanine residue, indicating that both the antibody in the resting form and the antibody–antigen complex become unstable in going from the wild type to the mutants. In case of N58A mutant, however, the binding affinity for the antigen increases because the antibody–antigen complex is destabilized to the less extent than the antibody in the resting form. On the other hand, the more destabilization of the antibody–antigen complex than the free antibody can be invoked to explain the reduced binding affinity of Y96A mutant for the preS1 antigen. Judging from the more negative values of ΔG_b than ΔG_u, the increase in binding affinities in going from the wild-type to D97A and D97A/Y102A mutants of HzKR127 can be attributed to the more stabilization of the antibody–antigen complex than the unliganded antibody during the structural transformations. This implies that to increase the efficacy of the antibody, the structural modification should be made in such a way that the resulting stabilization energy of the antibody–antigen complex overbalances that of the antibody itself in bulk solvent. Overall, the results of the present MD–FEP calculations for the relative binding free energies of the mutant antibodies are in good agreement with the experimental mutagenesis data; the associated squared correlation coefficient amounts to 0.96. MD–FEP calculations can thus be a valuable tool for elucidating the mutation-induced change in the binding affinities of HzKR127 antibody for the antigen, and therefore for the rational design of the mutant antibodies with increased efficacy.

Table 1
Calculated free energy changes in the virtual transformations of wild-type HzKR127 into its single or double mutants in the resting (ΔG_u) and in the antigen-bound form (ΔG_b), and relative binding free energies ($\Delta\Delta G_{bind}$). Experimental data for the mutation-induced change in binding free energies ($\Delta\Delta G_{exp}$) are also listed. All energy values are given in kcal/mol.

Mutants	ΔG_u	ΔG_b	$\Delta\Delta G_{bind}$	$\Delta\Delta G_{exp}$
N58A	+13.2 ± 0.3	+11.5 ± 0.2	−1.7 ± 0.4	−1.2
Y96A	+14.0 ± 0.2	+16.6 ± 0.1	+2.6 ± 0.2	+4.2
D97A	−10.1 ± 0.3	−11.4 ± 0.3	−1.3 ± 0.5	−1.8
D97A/Y102A	−17.3 ± 0.4	−19.7 ± 0.2	−2.4 ± 0.4	−1.9

We now turn to the identification of the mutation-induced structural changes in the antibody–antigen interactions that are responsible for the increase or decrease in binding affinity for the antigen. Fig. 6 compares the representative structures of MD–FEP trajectories of the wild type and N58A mutant of HzKR127 in complex with the antigen. These structures were prepared by the time-averages over the trajectories for the first (λ = 0) and the final (λ = 1) windows of perturbation that correspond to the wild-type and N58A mutant of HzKR127, respectively. The hydrogen bond interactions appear to be the most significant binding forces that stabilize the antigen in CDR of the wild-type and mutant antibodies. Among them, those involving the side chain of Arg50 in the heavy chain (Arg50H) seem to play a crucial role in binding of the antigen because it donates three hydrogen bonds to the side chain of an aspartate residue and the two backbone aminocarbonyl oxygens of the preS1 antigen. It is noteworthy that the time-averaged

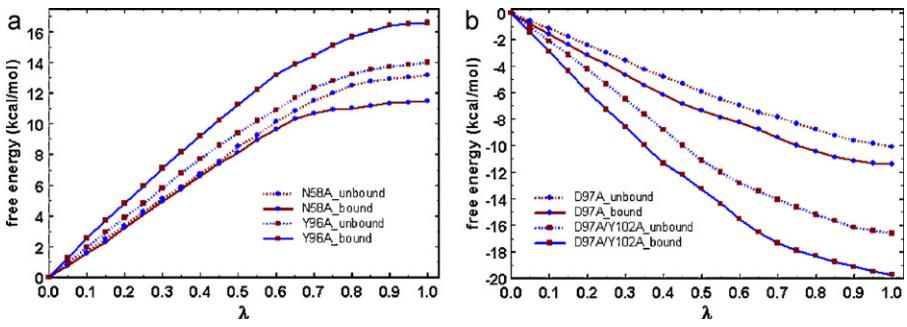

Fig. 5. Changes in free energy of binding with λ for the structural transformation of the wild-type HzKR127 to (a) N58A and Y96A mutants, and (b) D97A and D97A/Y102A mutants.

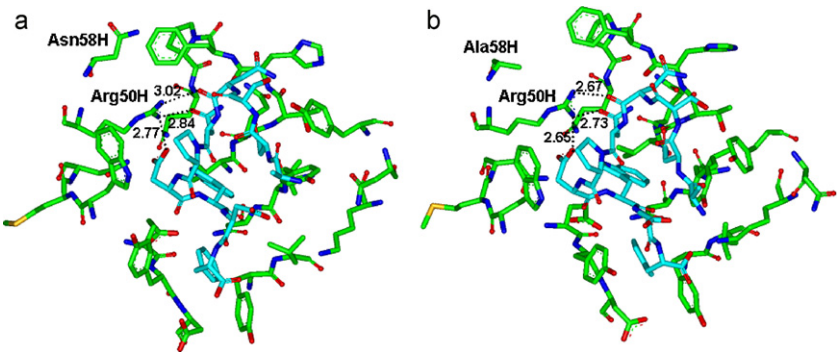

Fig. 6. Comparative view of the representative structures in the MD–FEP trajectories of HzKR127–preS1 complex for (a) wild type and (b) N58A mutant. Hydrogen atoms and solvent molecules are removed for clarity. Hydrogen bond distances are indicated in Å. (For interpretation of the references to color in this figure legend, the reader is referred to the web version of the article.)

interatomic distances associated with the three N–H···O hydrogen bonds decrease from 2.77, 2.84, and 3.02 Å in the wild type to 2.65, 2.73, and 2.67 Å, respectively, in N58A mutant. This indicates the strengthening of the hydrogen bonds due to the mutation from Asn to Ala residue at the position 58 in the heavy chain, which may be invoked to explain the increased binding affinity of N58A mutant for the antigen. The strengthening of the hydrogen-bond interactions between the Arg50H and the antigen in N58A mutant can be understood as compensation for the loss of some stabilizing interactions of the Arg50H in the antibody. Because Asn58H resides in the vicinity of Arg50H in the wild type, its change to the hydrophobic Ala residue would lead to the weakening of the inter-residue interactions between the Arg50H and the residue 58H. As a confirmation of this hypothesis, we calculated the average interatomic distance between CB atom of the residue 58H and the NZ atom of Arg50H for the wild type the mutant. The time-averaged distances have been found to be 4.64 and 5.29 Å in the wild type and N58A mutant of HzKR127 in complex with the preS1 antigen, respectively. This indicates the weakening of the interaction between the residues 58 and 50 in the heavy chain in going from the wild type to N58A mutant. The destabilized Arg50H in N58A mutant is thus likely to be capable of establishing the stronger hydrogen bonds with the antigen groups than those in the wild type.

Fig. 7 shows the representative structures in the MD–FEP trajectories for the wild-type and Y96A mutant of HzKR127 in complex with the antigen. It is seen that the side chain of the terminal phenylalanine residue of the antigen establishes the van der Waals contact with the phenolic groups of Tyr96H and Tyr54 in the light chain of HzKR127 (Tyr54L) in the wild type. In response to the Tyr → Ala mutation of the residue 96 in the heavy chain, however, the phenyl group of the antigen moves toward Ala96H, which leads to the change of its one of the interacting partners from the phenolic to the methyl moiety. Because the hydrophobic interactions between aromatic groups are stronger than the aromatic–aliphatic interactions [24], the mutation would have an effect of weakening the interaction of the antigen with the heavy-chain residue at the position 96. As a consequence of the positional shift of the phenyl moiety of the antigen, furthermore, it resides more distant from Tyr54L in Y96A mutant than in the wild type; the associated time-averaged minimum interatomic distance increases from 3.79 Å in the wild type to 4.08 Å in the mutant. The decrease in binding affinity for the antigen in Y96H mutant can thus be attributed to the weakening of the van der Waals interactions of the antigen with both heavy and light chain residues in CDR.

On the other hand, the hydrophobic interactions of the terminal phenylalanine of the antigen with the two Tyr residues of the antibody appear to get stronger in going from the wild type to D97A mutant. As can be seen in Fig. 7a, Asp97H of the wild type seems to make little contribution to the stabilization of the antigen in CDR of HzKR127 because its side chain points toward bulk solvent and stays distant from the antigen. This stems from the repulsive interaction between the two carboxylate groups of Asp97H and the peptide backbone C-terminal of the antigen. However, the change of Asp97 in the heavy chain to the hydrophobic alanine facilitates the interaction with the terminal phenylalanine of the antigen, and leads to the establishment of a van der Waals contact between the methyl and the phenyl moieties (Fig. 8a). It is apparent that this interaction should have an effect of stabilizing the antigen in

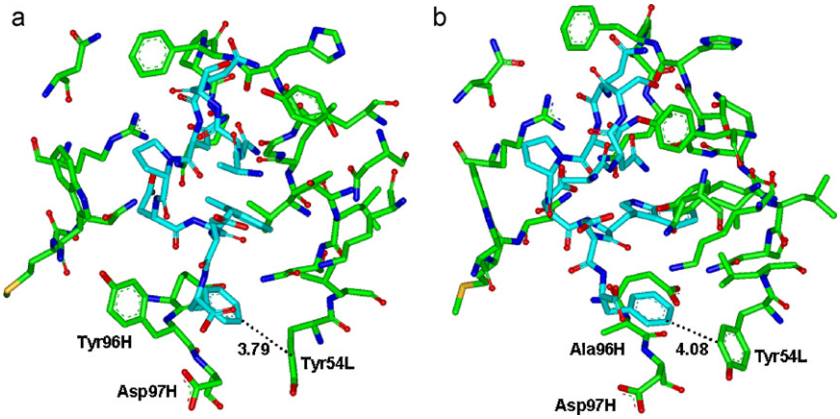

Fig. 7. Comparative view of the representative structures in the MD–FEP trajectories of HzKR127–preS1 complex for (a) wild type and (b) Y96A mutant. Interatomic distances associated with van der Waals interactions are indicated in Å. (For interpretation of the references to color in this figure legend, the reader is referred to the web version of the article.)

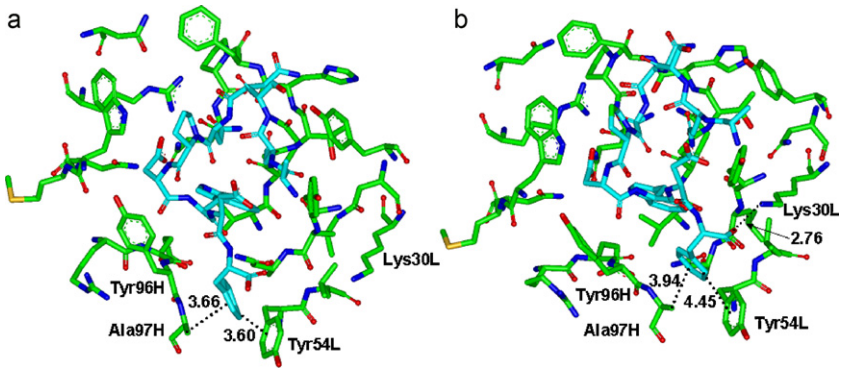

Fig. 8. Comparative view of the representative structures in the MD–FEP trajectories of HzKR127–preS1 complex for (a) D97A and (b) D97A/Y102A mutants. Interatomic distances associated with hydrogen bond and van der Waals interactions are indicated in Å. (For interpretation of the references to color in this figure legend, the reader is referred to the web version of the article.)

CDR, which is consistent with the experimental data indicating the enhancement of antigen binding in going from the wild type to D97A mutant of HzKR127. Therefore, the enlargement of the residue 97 to a more hydrophobic residue such as Leu, Ile, and Phe is expected to cause the increase in the efficacy of HzKR127 through the promotion of the hydrophobic interactions with the antigen. It is also noteworthy that the time-averaged distance between the two phenyl groups belonging to the terminal phenylalanine of the antigen and the Tyr54L of the antibody contracts from 3.79 Å in the initial state (wild type of HzKR127, Fig. 7a) to 3.60 Å in the final state (D97A mutant, Fig. 8a) of MD–FEP simulations. This indicates that due to a proper positioning of the terminal phenylalanine of the antigen by Ala97H, it can be further stabilized in CDR of D97A mutant by strengthening the existing aromatic hydrophobic interaction with Tyr54L. Thus, the terminal phenylalanine of the antigen can be accommodated in a small hydrophobic pocket in CDR of D97A mutant, which can be attributed to its higher binding affinity for the antigen than the wild type.

An additional mutation at the position 102 in the heavy chain from tyrosine to alanine should have an effect of moving CDR from the exterior to the core of the heavy chain because Y102H resides at the bottom of CDR with its phenolic group flipping in the opposite direction of the antigen [16]. As a consequence of this structural contraction, the hydrophobic interactions of the terminal phenylalanine of the antigen with Ala97H and Tyr54L undergoes a weakening to a significant extent in D97A/Y102A mutant, which is reflected in lengthening of the associated time-averaged interatomic distances from 3.66 and 3.60 Å in D97A mutant to 3.94 and 4.45 Å in D97A/Y102A mutant (Fig. 8). However, the separation of the terminal phenylalanine residue from the hydrophobic residues in CDR causes its approach to Lys30 in the light chain of the antibody. This leads to the formation of a strong hydrogen bond between the terminal backbone carboxylate group of the antigen and the ammonium-ion side chain of Lys30L: the time-averaged distance from the NZ atom of Lys30L to the terminal carboxylate atom decreases to a substantial extent from 6.18 Å in D97A to 2.76 Å in D97A/Y102A mutant. Judging from a little higher binding affinity of D97A/Y102A mutant for the antigen than D97A mutant, the hydrogen-bond stabilization of the terminal backbone carboxylate group of the antigen seems to be sufficient to compensate for the weakening of the hydrophobic interactions with the nonpolar residues.

On the basis of the energetic and structural features of antigen binding for the mutant antibodies found with MD–FEP simulations, some new mutants that are likely to have enhanced binding affinity for the preS1 antigen can be proposed. Because the positions of the residues 58 and 97 are distant from each other, N58A/D97A double mutant is expected to have better efficacy than the two single mutants due to the simultaneous strengthening of the hydrogen-bond and the hydrophobic interactions with the antigen. The changes of the residues in D97A/Y102A mutant from Ala97H and Tyr54L to those with an increased volume would make it possible for the terminal carboxylate group of the antigen to form the hydrogen bond with the side chain of Lys30L without a significant loss of the hydrophobic interactions of the terminal phenylalanine of the antigen with the antibody. For example, D97F/Y102A and Y54W/D97A/Y102A mutants seem to have an enhanced binding affinity for the antigen. Although the triplet N58A/D97A/Y102A mutant can also be considered to have an increased efficacy in terms of the simultaneous strengthening of the hydrogen bond and hydrophobic interactions with the antigen, it may have poor physical properties due to the change of too many hydrophilic residues to hydrophobic ones in the exterior of the antibody. Therefore, the engineering of HzKR127 antibody should be approached with caution considering the compromise between the strengthening of the interaction with the antigen and the maintenance of good physicochemical properties.

4. Conclusions

We have examined the mutational changes in the structural and energetic features associated with the interaction of HzKR127 antibody with the preS1 antigen by means of the MD-based FEP calculations. For the four mutants under investigation, it is found that the extent of the positional shift of the antigen in CDR of the antibody should be less than that of the conformational change of the antibody. The increased binding affinity in N58A, D97A, and D97A/Y102A mutants can be attributed either to the more stabilization or to the less destabilization of the antibody–antigen complex than the antibody in the resting form in going from the wild type to a mutant. Comparison of the patterns for the interactions of the wild-type and mutant antibodies with the antigen shows that the strengthening of the existing hydrogen-bond and van der Waals interactions should be responsible for the increased binding affinities of N58A and D97A mutants, respectively. By contrast, the preS1 antigen appears to gain extra stabilization energy due to the formation of a new hydrogen bond upon binding to D97A/Y102A mutant. Consistent with the lower efficacy of Y96A mutant than the wild type, the antigen is found to be destabilized in CDR of the mutant due to the weakening of hydrophobic interactions with the antibody. FEP calculations are thus found to be very useful for elucidating the mutation-induced change in binding affinity of HzKR127 antibody for the preS1 antigen. The predicted differential binding modes and binding free energies of the antigen in CDR of various mutant antibodies are expected to provide useful information for the rational design of new antibody for neutralizing HBV.

Acknowledgements

This work was supported by Grant No. M1071130000208M113000210 from Pioneer Research Program for Converging Technology of Korea Science & Engineering Foundation (granted to HP), and by NMR research program of Korea Basic Science Institute (granted to YHJ).

References

[1] B. Rehermann, M. Nascimbeni, Immunology of hepatitis *B* virus and hepatitis C virus infection, Nat. Rev. Immunol. 5 (2005) 215–229.
[2] K.H. Heermann, U. Goldmann, W. Schwartz, T. Seyffarth, H. Baumgarten, W.H. Gerlich, Large surface proteins of hepatitis B virus containing the pre-S sequence, J. Virol. 52 (1984) 396–402.
[3] M. Nassal, Hepatitis B viruses: reverse transcription a different way, Virus Res. 134 (2008) 235–249.
[4] S. De Falco, M.G. Ruvoletto, A. Verdoliva, M. Ruvo, A. Raucci, M. Marino, S. Senatore, G. Cassani, A. Alberti, P. Pontisso, G. Fassina, Cloning and expression of a novel hepatitis B virus-binding protein from HepG2 cells, J. Biol. Chem. 276 (2001) 36613–36623.
[5] C.Y. Maeng, C.J. Ryu, P. Gripon, C. Guguen-Guillouzo, H.J. Hong, Fine mapping of virus-neutralizing epitopes on hepatitis B virus preS1, Virology 270 (2000) 9–16.
[6] H.J. Hong, C.J. Ryu, H. Hur, S. Kim, H.K. Oh, M.S. Oh, S.Y. Park, In vivo neutralization of hepatitis B virus infection by an anti-preS1 humanized antibody in chimpanzees, Virology 318 (2004) 134–141.
[7] M. Verhoeyen, C. Milstein, G. Winter, Reshaping human antibodies: grafting an antilysozyme activity, Science 239 (1988) 1534–1536.
[8] S. Stephens, S. Emtage, O. Vetterlein, L. Chaplin, C. Bebbington, A. Nesbitt, M. Sopwith, D. Athwal, C. Novak, M. Bodmer, Comprehensive pharmacokinetics of a humanized antibody and analysis of residual anti-idiotypic responses, Immunology 85 (1995) 668–674.
[9] L. Riechmann, M. Clark, H. Waldmann, G. Winter, Reshaping human antibodies for therapy, Nature 332 (1988) 323–327.
[10] M.S. Co, M. Deschamps, B.J. Whitley, C. Queen, Humanized antibodies for antiviral therapy, Proc. Natl. Acad. Sci. U.S.A. 88 (1991) 2869–2873.
[11] M.S. Co, N.M. Avdalovic, P.C. Caron, M.V. Avdalovic, D.A. Scheinberg, C. Queen, Chimeric and humanized antibodies with specificity for the CD33 antigen, J. Immunol. 148 (1992) 1149–1154.
[12] S.A. Marshall, G.A. Lazar, A.J. Chirino, J.R. Desjarlais, Rational design and engineering of therapeutic proteins, Drug Discov. Today 8 (2003) 212–221.
[13] D.J. Mandell, T. Kortemme, Computer-aided design of functional protein interactions, Nat. Chem. Biol. 5 (2009) 797–807.
[14] H. Fazelinia, P.C. Cirino, C.D. Maranas, Extending iterative protein redesign and optimization (IPRO) in protein library design for ligand specificity, Biophys. J. 92 (2007) 2120–2130.
[15] M. Berrondo, J.J. Gray, R. Schleif, Computational predictions of the mutant behavior of AraC, J. Mol. Biol. 398 (2010) 462–470.
[16] S.W. Chi, C.Y. Maeng, S.J. Kim, M.S. Oh, C.J. Ryu, S.J. Kim, K.H. Han, H.J. Hong, S.E. Ryu, Broadly neutralizing anti-hepatitis B virus antibody reveals a complementarity determining region H3 lid-opening mechanism, Proc. Natl. Acad. Sci. U.S.A. 104 (2007) 9230–9235.
[17] G.A. Jeffrey, An Introduction to Hydrogen Bonding, Oxford University Press, Oxford, 1997.
[18] D.A. Case, T.E. Cheatham III, T. Darden, H. Gohlke, R. Luo, K.M. Merz Jr., A. Onufriev, C. Simmerling, B. Wang, R.J. Woods, The Amber biomolecular simulation programs, J. Comput. Chem. 26 (2005) 1668–1688.
[19] W.D. Cornell, P. Cieplak, C.I. Bayley, R. Gould, K.M. Merz Jr., D.M. Ferguson, D.C. Spellmeyer, T. Fox, J. Caldwell, P.A. Kollman, A second-generation force field for the simulation of proteins, nucleic acids, and organic molecules, J. Am. Chem. Soc. 117 (1995) 5179–5197.
[20] W. Jorgensen, J. Chandrasekhar, J. Madura, R. Impey, M. Klein, Comparison of simple potential functions for simulating liquid water, J. Chem. Phys. 79 (1983) 926–935.
[21] H.J.C. Berendsen, J.P.M. Postma, W.F. van Gunsteren, A. DiNola, J.R. Haak, Molecular dynamics with coupling to an external bath, J. Chem. Phys. 81 (1984) 3684–3690.
[22] J.P. Ryckaert, G. Ciccotti, H.C. Berendsen, Numerical integration of the Cartesian equations of motion of a system with constraints: molecular dynamics of n-alkanes, J. Comput. Phys. 23 (1977) 327–341.
[23] W. Jiang, M. Hodoscek, B. Roux, Computation of absolute hydration and binding free energy perturbation distributed replica-exchange molecular dynamics, J. Chem. Theory Comput. 5 (2009) 2583–2588.
[24] H.J. Böhm, The development of a simple empirical scoring function to estimate the binding constant for a protein–ligand complex of known three-dimensional structure, J. Comput.-Aided Mol. Design 8 (1994) 243–256.